JOURNAL OF AGRICULTURAL AND FOOD CHEMISTRY

Solving the Spectroscopy Interference Effects of β-Carotene and Lycopene by Neural Networks

JOSÉ S. TORRECILLA,† MONTAÑA CÁMARA,‡ VIRGINIA FERNÁNDEZ-RUIZ,‡ GUIOMAR PIERA,‡ AND JORGE O. CACERES*,§

Departamentos de Ingeniería Química and Química Analítica, Facultad de Ciencias Químicas, and Departamento de Nutrición y Bromatología II, Facultad de Farmacia, Universidad Complutense de Madrid, Avenida Complutense s/n, 28040 Madrid, Spain

In this study a new computerized approach and linear models (LMs) to solve the UV/vis spectroscopy interference effects of β-carotene with lycopene analysis by neural networks (NNs) are considered. The data collected (absorbance values) obtained by UV/vis spectrophotometry were transferred into an NN-trained computer for modeling and prediction of output. Such an integrated NN/UV/vis spectroscopy approach is capable of estimating β-carotene and lycopene concentrations with a mean prediction error 50 times lower than that calculated by the LM/UV/vis spectroscopy approach (without any previous physicochemical knowledge of the process to be modeled).

KEYWORDS: β-Carotene; lycopene; chemical interferences; neural networks; UV spectroscopy

INTRODUCTION

Carotenoids are widespread in nature, being the main group of pigment with important metabolic functions (*1*). There are many studies showing strong correlation between carotenoid intake and a reduced risk of some diseases, such as cancer, atherogenesis, bone calcification, eye degeneration, and neuronal damages (*2–4*), due its antioxidant activity.

The analytical methods for measuring carotenoids in vegetables are limited due to their characteristics of solubility and instability, which makes necessary a very careful handling process and a short analysis time to avoid degradation and isomerization. For this reason, the necessity for a reliable and rapid analysis method for carotenoid quantification in vegetable products is recognized in the literature (*5, 6*). Carotenoid analysis in food products may be done by different analytical methods such as high-performance liquid chromatography (HPLC), spectrophotometry, or color evaluation (*7, 8*). A spectroscopy method for carotenoid analysis is faster, cheaper, and easier to perform than an HPLC method which is more time-consuming and requires specific reagents, complex instrumentation, and more trained people to perform the analysis. The selection of an analytical method depends on the accuracy requirements, analysis conditions (sampling time, sample preparation, etc.), and the kind of product analyzed (physicochemical stability, solubility, etc.) (*8, 9*). In spite of the great interest in both β-carotene and lycopene analysis, better methods for their characterization and determination are still needed (*10*).

Spectrophotometry can be used to rapidly assess the β-carotene and lycopene contents of different vegetable products; this method shows an overestimation of the carotenoid content as has been demonstrated in a previous study by Olives Barba et al. (*9*). These authors showed the overlap of the lycopene band at 446 nm with that of β-carotene as the main reason for the observed deviations, compared with the resolution obtained by HPLC. The differences in the absorption spectrum between lycopene and other major carotenoids in foods such as α-carotene, β-carotene, or luteine make the lycopene quantification easy at its characteristic maximum of 502 nm, with no interference from other compounds, in lycopene-rich samples such as tomato or watermelon. Fish et al. (*11*) stated that, in samples where lycopene is at least 70% of the constituent carotenoids, the contribution of carotenoids other than lycopene to the absorbance at 502 nm is less than 2% for watermelon, 4% for tomato, and 6% for pink grapefruit. This problem is almost nonexistant in tomato products where lycopene is the mayor carotenoid (*12*). However, in samples where lycopene is less than 70%, using these absorbance values, the carotenoid quantification is notably less accurate.

Given the complexity of an adequate resolution of the UV/vis spectra mentioned previously together with the need for a quick and precise determination of each one, it is necessary to develop techniques capable of solving the interferences of these chemical compounds.

Algorithms based on neural networks (NNs) fulfill these requirements; they can be used to resolve complex spectra and interferences between different compounds. NNs have been applied to the interpretation of voltamperometric measurement of glucose and ascorbic and uric acid mixtures (*13*) as well as

* To whom correspondence should be addressed. E-mail: jcaceres@quim.ucm.es. Fax: +34-913944329.

† Departamento de Ingeniería Química, Facultad de Ciencias Químicas.

‡ Departamento de Nutrición y Bromatología II, Facultad de Farmacia.

§ Departamento de Química Analítica, Facultad de Ciencias Químicas.

10.1021/jf8005239 CCC: $40.75
Published on Web 07/04/2008

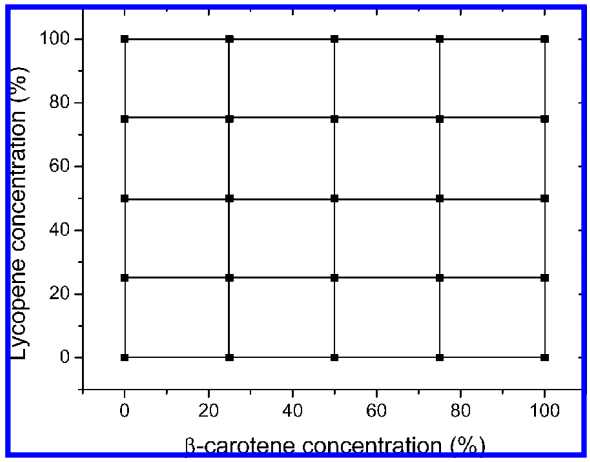

Figure 1. Five-level factor experimental design of two factors and two response variables used to optimize the neural network.

UV/vis spectra of 1-ethyl-3-methylimidazolium ethyl sulfate, toluene, and water mixtures, obtaining satisfactory results (*14*). NNs have been recently applied to different aspects of food science such as the interpretation of spectroscopic data, identification of functional groups, and quantitative analysis (*15*). At the present, no work has been reported on the resolution of carotenoid spectra.

In this work, an NN/UV/vis approach was used to determine the β-carotene and lycopene concentrations from standard mixtures. The spectral information obtained by spectrophotometry (measurement of the absorption intensity) was used as an input vector, and the analyte concentration was used as an output vector. The present results may open the way to other applications in the treatment of data for the resolution of complex spectra as UV/vis determination of carotenoids in foods.

MATERIALS AND METHODS

Reagents, Standards, and Instrumentation. Standards of *all-trans*-lycopene and β-carotene used in this work were from Sigma-Aldrich-Fluka (St. Louis, MO), with a purity ≥90%. Standard solutions of known amounts of β-carotene and lycopene in *n*-hexane (Merk, Darmstadt, Germany) were prepared every day. Their absorptivities were compared to check their purity by calculating the real concentration of the standard solution using the extinction coefficient (*16, 17*).

Standard Mixtures. For identification and quantification purposes individual working standard solutions in the range of 0.4−3.2 $\mu g \cdot mL^{-1}$ were freshly prepared by dilution in hexane. A five-level factor experimental design of two factors and two response variables was performed to optimize the neural network model. These factors were β-carotene and lycopene concentration values, in the range between 0.4 and 1.6 $\mu g \cdot mL^{-1}$. The response variables were the absorbance values at 446 nm for β-carotene and 502 nm for lycopene. The percentages of β-carotene and lycopene of each experimental mixture designed (25 in total) are shown in **Figure 1**.

A Pharmacia Ultrospec 4000 UV/vis spectrophotometer was employed for absorbance measurements using quartz cells of path length 1 cm. Data acquisition and spectrometric evaluation were performed using PESSW software, version 1.2. In all cases, a minimum of three replicate measurements of spectroscopic absorption for each sample were carried out.

Neural Network Model. In this work, a multilayer feed forward neural network, specifically a back-propagating perceptron model, has been used. This model has been successfully applied to a variety of practical pattern recognition tasks, signal filtering (*18*), modeling and control (*19, 20*), and estimation of chemical concentrations, solving their interferences (*13, 14*).

The NN used consisted of three layers called the input, hidden, and output layers, and they consisted of neurons (single operating elements). The input layer was only used to input the database into the NN. In the other layers, nonlinear calculations were performed. In the hidden layer, each neuron received signals from other input neurons (neurons in the input layer); these signals were summed by the activation function, eq 1. Then, the result was transformed by the transfer function, eq 2. Finally, the result was sent to the output neurons (neurons in the output layer). In every output neuron, after similar calculations (vide supra), the estimations were calculated. In eqs 1 and 2, y_j and y_k represent the output of hidden (j) and output (k) neurons, respectively. w_{jk} represents the weight between the jth hidden and the kth output neurons. Hyperbolical tangent, sigmoid, or linear algorithms are commonly used as transfer functions (*21*). As the sigmoid algorithm, eq 2, and the data used here ranged between 0 and 1, this algorithm was used as the transfer function. The weights were adjustable parameters of the NN associated with each of the connections between neurons, and they modified the communicated signal between neurons (*19*).

$$x_k = \sum_{j=1} w_{jk}\, y_j \tag{1}$$

$$y_k = f(x_k) = \left(\frac{1}{1+e^{-x_k}}\right) \tag{2}$$

The optimization process of the NN matrix of weights was carried out by the training function. Here, the training function was selected to prevent the overfitting (violation of Occam's razor) and overtraining (*22*). The overtraining problem referred to the fact that the network only memorized the learning set and lost its ability to generalize. With few learning samples, the Bayesian regularization back-propagation model (TrainBR) was selected to perform the learning process because its generalization power was higher than that of other training functions (*23*). TrainBR minimized the prediction error by using a linear combination of mean square estimation error (MSE), eq 3, and weight (MSW), eq 4. It determined the correct combination to produce a network that generalized new input data well inside the learning data range. In eqs 3 and 4, N, y_k, r_k, and w are the number of observations, NN model estimation, real value, and weight value between layers and the subscripts i, j, and k indicate the input, hidden, and output layers, respectively. In eq 5, γ is the performance ratio, which was set to 0.5, giving equal importance to MSE and MSW values (*23*).

$$\mathrm{MSE} = \frac{1}{N}\sum_{k}^{N}(r_k - y_k)^2 \tag{3}$$

$$\mathrm{MSW} = \frac{1}{N}\left[\sum_{i}^{N}\sum_{j} w_{ij}^{\,2} + \sum_{j}^{N}\sum_{k} w_{jk}^{\,2}\right] \tag{4}$$

$$\mathrm{msereg} = \gamma(\mathrm{MSE}) + (1-\gamma)(\mathrm{MSW}) \tag{5}$$

The TrainBR algorithm was used to update the matrix of weight according to the Levenberg−Marquardt optimization. The Jacobian jX of performance with respect to the weight and bias variables X was calculated in the back-propagation calculation procedure:

$$jj = jX \cdot jX \tag{6}$$

$$j\mathbf{e} = jX \cdot \mathbf{e} \tag{7}$$

$$\mathrm{d}X = -\frac{jj + \mathbf{I}\cdot \mathrm{Lc}}{j\mathbf{e}} \tag{8}$$

In eqs 7 and 8, **e** is a vector of network errors, Lc and **I** are the learning coefficient (similar to the h parameter in Newton's method, often called the Newton−Raphson method or the Newton-Fourier method) and identity matrix, respectively. If the msereg value, eq 5, decreases or increases, Lc also goes down or up by a learning coefficient decrease (Lcd) or learning coefficient increase (Lci) parameter, respectively.

The topology of the NN used here consisted of an input layer with two neurons for the input variables (absorbance at 502 and 446 nm), one hidden layer (optimized afterward), and an output layer with two neurons to estimate β-carotene and lycopene concentration values. This topology with a single hidden layer was suitable to solve problems of similar or even higher complexity (*19, 24, 25*). Moreover, more hidden layers may have

Table 1. Calibration Parameters and Sensibility of the UV/Vis Spectrophotometric Method Applied to Lycopene and β-Carotene[a]

	equation	interval ($\mu g \cdot mL^{-1}$)	R^2	σ intercept	σ slope	LOD[b] (μg)	LOQ[c] (μg)
lycopene	$Abs_{502} = 0.200[C\ (\mu g \cdot mL^{-1})] - 0.001$	0.4−3.2	>0.999	0.002	0.001	0.04	0.11
β-carotene	$Abs_{446} = 0.252[C\ (\mu g \cdot mL^{-1})] - 0.001$	0.4−3.2	>0.999	0.003	0.002	0.04	0.13

[a] σ = standard deviation, LOD = limit of detection, and LOQ = limit of quantification. [b] Equation 10. [c] Equation 11.

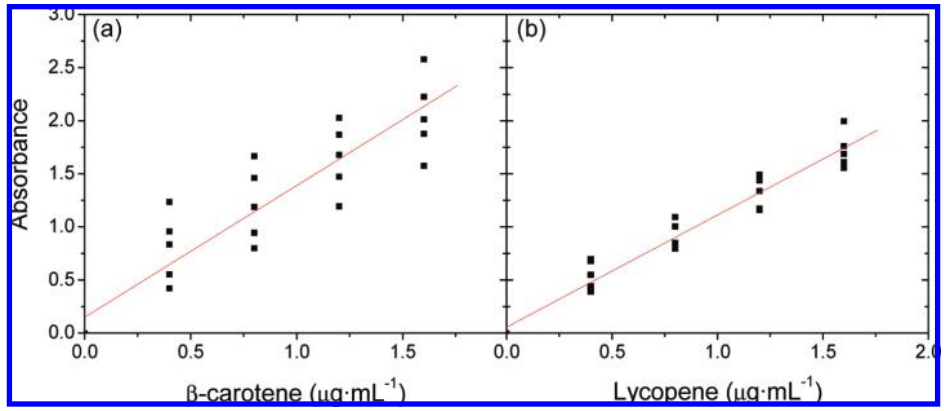

Figure 2. Mixing standard sample absorbance values at 502 and 446 nm for β-carotene (**a**) and lycopene (**b**), respectively.

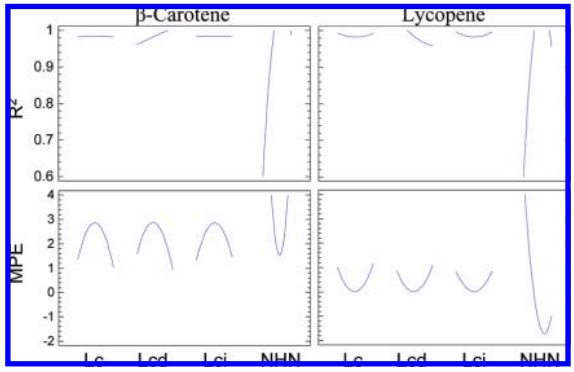

Figure 3. Analysis of the influence of factors (Lc, Lcd, Lci, NHN) on the responses in the experimental design.

Table 2. Parameters and Characteristics of the Optimized NN Model

NN Model Characteristics	
transfer function	sigmoid function
training function	TrainBR

Optimized Parameters of the NN Model	
input neuron number	2
hidden neuron number	5
output neuron number	2
learning coefficient	0.32
learning coefficient decrease	0.67
learning coefficient increase	57

caused overfitting, since the network focused excessively on the idiosyncrasies of individual samples (*25*). Every NN model used in this work was designed using Matlab, version 7.01.24704 (R14). The statistical analyses were carried out by Statgraphics Plus, version 5.1.

Learning and Verification Samples and Processes. (a) Learning and Verification Samples. Given that the NN used was based on a supervised algorithm, to optimize the matrix of weights, it was necessary to use input and output data that adequately characterize the process to be modeled. These data were obtained with the experimental design described in the "Reagents, Standards, and Instrumentation" section. These data were divided into two groups, viz., learning and verification samples. In this work, the data were organized in four rows (absorbance at 502 and 446 nm and their respective β-carotene and lycopene concentration values). The whole data set (absorbance values of 25 β-carotene and lycopene mixtures) was randomly distributed into the learning (80%) and verification (20%) samples, but taking into account that no data set or any of its replications must be presented in the verification sample.

Table 3. Main Statistical Results of the Linear and NN Models Corresponding to the Verification Samples

	β-carotene		lycopene	
	linear	NN	linear	NN
mean PV	0.09	0.817	0.15	0.843
MPE ($\mu g \cdot mL^{-1}$)	1.86	0.02	1.10	0.04
R^2	0.596	0.991	0.970	0.999
standard deviation ($\mu g \cdot mL^{-1}$)	0.54	0.03	0.46	0.04

(b) Learning and Verification Processes. The learning process was the mathematical procedure used to optimize the matrix of weights. It was carried out by presenting the learning samples to the NN model. When the output was estimated, the MSE value was calculated, eq 3. Then the back-propagation algorithm was applied to optimize the matrix of weights of the NN as a function of MSE. This calculation process has been described in the literature (*19, 21, 24*).

In the verification process, when the weights were optimized, using the absorbance values at 446 and 502 nm (input variables of the verification sample), the β-carotene and lycopene concentration values were estimated. Then these values were statistically compared with the experimental β-carotene and lycopene concentrations (output variables of verification samples). The statistical comparison was carried out by the mean prediction error (MPE; eq 9), correlation coefficient (R^2), and p value (PV) between the estimated and experimental values. PV was a result of the statistical analyses. If PV > 0.05, the estimated and experimental databases can be assumed statistically equal (null hypotheses), and the higher the PV value, the more evidence that exists of null hypotheses. In eq 9, N, y_k, and r_k are the number of observations, NN model estimation, and real value, respectively.

$$\mathrm{MPE} = \frac{1}{N}\sum_{k} |r_k - y_k| \qquad (9)$$

Optimization Process of the Neural Network Model. Given that the designed NN was used to estimate the β-carotene and lycopene concentration values with the best statistical parameters (MPE, R^2, and PV) as possible, the NN used must be optimized. The optimization process consists of two stages: first, the main parameters of the NN were optimized, and second, the optimized NN was tested using the verification sample.

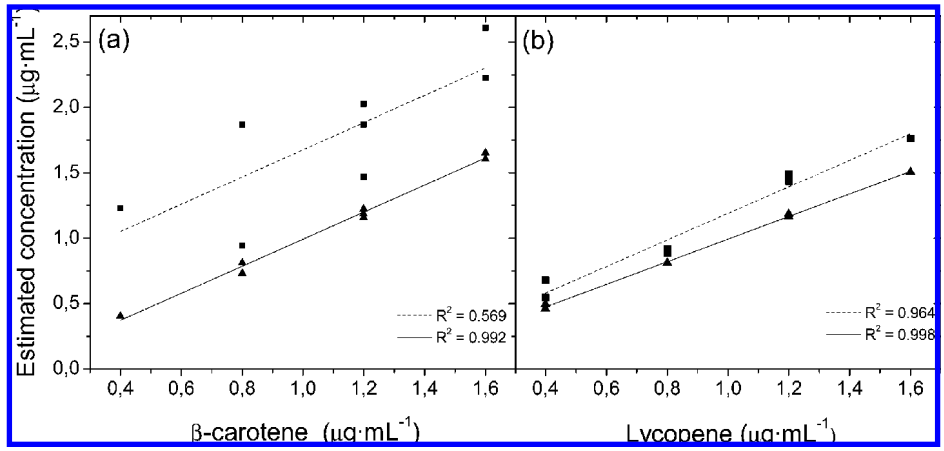

Figure 4. Estimation of the β-carotene (**a**) and lycopene (**b**) concentrations from linear (■) and nonlinear (▲) models versus their experimental concentration values and their best fit lines (dashed and solid, respectively).

Table 4. Validation of the Neural Network Using Real Samples[a]

	β-carotene concn ($\mu g \cdot mL^{-1}$)		lycopene concn ($\mu g \cdot mL^{-1}$)	
sample	experimental (LM)	estimated (NN)	experimental (LM)	estimated (NN)
tomato concentrate	1.004	1.032	1.955	1.969
	1.536	1.643	2.798	2.741
tomato sauce	0.881	0.941	1.711	1.639
	0.909	0.889	1.591	1.637
ketchup	0.964	0.970	1.706	1.769
	0.778	0.731	1.461	1.512
tomato juice	0.699	0.679	1.401	1.457
	0.675	0.700	1.192	1.142
tomato puree	0.663	0.665	1.272	1.312
	1.536	1.594	2.818	2.867
		Statistical Results		
MPE[b] ($\mu g \cdot mL^{-1}$)		0.04		0.05
R^2		0.992		0.991

[a] Experimental values calculated by the linear method (LM) and estimated values obtained by the NN application. [b] Equation 9.

(a) Optimization of the NN Parameters. Given that TrainBR was used as a training function, the main parameters to optimize were the number of hidden neurons (NHN), Lc, Lcd, and Lci. The optimization process was carried out by a central composite design 2^4 + star experimental design, where the variables analyzed were the parameters to optimize. Its responses were MPE, R^2, and PV values. These were calculated using experimental and estimated concentration values.

The hidden neurons were tested between 1 and 10 neurons. As described below, NNs with a hidden neuron were not able to reproduce the process to be modeled. On the other hand, taking the number of training samples into account, 10 hidden neurons were estimated in the literature (*26*). Lci ranged between 2 and 100 and Lc and Lcd between 0.001 and 1 as was tested by Torrecilla et al. (*21*). The experimental design was analyzed taking into account that the NN should predict the β-carotene and lycopene concentrations with the lowest MPE, R^2, and PV values to be as close as possible to unity, in the lowest iteration number.

(b) Testing the Optimized NN. Finally, the verification sample was input into the optimized NN model, and its estimations were also statistically checked by calculating MPE, PV, and R^2 of the estimated versus experimental concentration values.

RESULTS AND DISCUSSION

Three types of model groups have been tested: two linear models (for β-carotene and lycopene compounds) and a model based on a neural network.

Linear Model. Using individual standard concentrations of β-carotene and lycopene (from 0.4 to 3.2 $\mu g \cdot mL^{-1}$) and their respective absorbance values at 502 and 446 nm, two calibration equations were obtained, **Table 1**. The calibration parameters and sensibility of the spectrophotometric methods applied to β-carotene and lycopene are also shown in **Table 1**. The detection (LOD) and quantification (LOQ) limits for this analytical method have been estimated following ICH Guideline Q2B (*27*), eqs 10 and 11, where S and m are, respectively, the intercept and slope of the fit equations.

$$\mathrm{LOD} = \frac{3S}{m} \tag{10}$$

$$\mathrm{LOQ} = \frac{10S}{m} \tag{11}$$

The β-carotene and lycopene concentrations from each of the 25 standard mixtures were quantified by the equations shown in **Table 1**. Interferences on the determination of the concentration of one compound by the presence of the other were found, **Figure 2**. The degree of uncertainty of the concentration of one compound was dependent on the concentration of the other. Given the interference between both compounds, the linear calibration models were not adequate to quantify them. To overcome this UV interference, a nonlinear model based on an NN was tested.

Neural Network Model Optimization. NHN, Lc, Lcd, and Lci were optimized following the process described in the "Learning and Verification Samples and Processes" section.

MPE and R^2 (real versus estimated values) versus Lc, Lcd, and Lci are plotted in **Figure 3**. The most significant parameter on the NN model performance was NHN. To reach the highest values of R^2 and minimize the MPE value, the Lc, Lcd, and Lci values were found to be about in the middle of the respective tested ranges. The optimized parameter values of the NN model are shown in **Table 2**.

To explore the NN model performance, using the verification samples, the model was used to predict the β-carotene and lycopene concentrations. The values of MPE, R^2, and σ and the mean PV of the estimated versus experimental values were calculated, **Table 3**.

PV was calculated with different parametric and nonparametric tests based on measures of central tendency (Kolmogorow−Smirnov test, Mann−Whitney−Wilcoxon test, and Kruscal−Wallis test) and on the dispersion (Kruscal−Wallis test, Cochran *C* test, Barllet's test, and Levene test) and inferential parametric tests for significance (*F* test and *t* test) (*24*). Although the mean PV value calculated comparing the estimated and experimental values of the lycopene concentration was the closest to 1, keeping both mean PV values (>0.8) in mind, the NN model estimations and experimental databases can be assumed as statistically equal.

Comparing the estimated β-carotene and lycopene concentration values, using linear models and the optimized NN model, R^2 increases from 0.596 and 0.970 (for β-carotene and lycopene) to 0.991 and 0.999, respectively. In addition, MPE decreases from 1.86 to 0.02 $\mu g \cdot mL^{-1}$ for β-carotene and from 1.10 to 0.04 $\mu g \cdot mL^{-1}$ for lycopene. σ and the mean PV by the NN model were better than those obtained with the linear model, **Table 3** and **Figure 4**.

Application of the Neural Network to Real Cases. Finally, to validate the prediction capability of the optimized NN, a new validation sample based on real samples (tomato concentrate, tomato sauce, ketchup, tomato puree, and tomato juice) was performed after carotenoid extraction on hexane (*9*). Tomato products were chosen due to their high lycopene content together with the presence of β-carotene. The mathematical procedure followed was similar to the verification process described above. In **Table 4** are included the results for tomato product analyses as well as β-carotene and lycopene statictical results, $R^2 > 0.99$ and MPE < 0.05. The optimized NN was able to estimate the β-carotene and lycopene concentrations with an adequate accuracy, when the NN was used within the range studied in comparison with the calibration curve analytical result method. Therefore, for the concentration range studied (0.4−1.6 $\mu g \cdot mL^{-1}$), the interference problems between β-carotene and lycopene can be adequately solved by the neural network.

Concluding Remarks. In this work, the measurement of the β-carotene and lycopene concentrations with different β-carotene and lycopene standard mixtures has been carried out using the spectrophotometric absorbance values at 446 and 502 nm, combined with an optimized neural network. To optimize the NN model, spectral information was used as an input vector and the analyte concentration was used as an output vector.

The neural network was capable of estimating the β-carotene and lycopene concentrations with a mean prediction error lower than 0.02 and 0.04 $\mu g \cdot mL^{-1}$, respectively. Using an NN model, the MPE value decreased 93 and 28 times with respect to the estimations of the β-carotene and lycopene concentrations calculated by linear models; therefore, the UV interference of β-carotene and lycopene can be solved using this NN model.

To conclude, we consider that the NN model applied was an adequate tool to determine accurately the β-carotene and lycopene concentrations in complex mixtures using a common analytical and simple technique such as UV/vis spectroscopy, avoiding the interferences and overestimation of traditional calibration methods. Once the carotenoids are extracted (sample preparation), the time required for their spectroscopy determination is considerably smaller (less than 15 min including the equipment calibration time) than that of HPLC analysis. With this method, extracted carotenoids have to be evaporated and redissolved in the appropriate mixture depending on the mobile phase composition and then injected into the HPLC system. After the neural network has been optimized, the analysis of the absorbance values would be on the order of seconds. This improvement in the result interpretations will be very valuable for its application to a fast and reliable β-carotene and lycopene evaluation in food samples.

LITERATURE CITED

(1) Goodwin, T. W. Metabolism, Nutrition, and Function of Carotenoids. *Annu. Rev. Nutr.* **1986**, *6*, 273–297.

(2) Cantuti-Castelvetri, I.; Shukitt-Hale, B.; Joseph, J. A. Neurobehavioral aspects of antioxidants in aging. *Int. J. Dev. Neurosci.* **2000**, *18*, 367–381.

(3) Ferguson, L. R. Micronutrients, dietary questionnaires and cancer. *Biomed. Pharmacother.* **1997**, *51*, 337–344.

(4) Yamaguchi, M.; Uchiyama, S. Effect of carotenoid on calcium content and alkaline phosphatase activity in rat femoral tissues in vitro: the unique anabolic effect of beta-cryptoxanthin. *Biol. Pharm. Bull.* **2003**, *26*, 1188–1191.

(5) Schoefs, B. Chlorophyll and carotenoid analysis in food products. Properties of the pigments and methods of analysis. *Trends Food Sci. Technol.* **2002**, *13*, 361–371.

(6) Bicanic, D.; Anese, M.; Luterotti, S.; Dadarlat, D.; Gibkes, J.; Lubbers, M. Rapid, accurate and direct determination of total lycopene content in tomato paste. *Rev. Sci. Instrum., Part 2* **2003**, *74* (1), 687–689.

(7) Sander, L. C.; Sharpless, K. E.; Pursch, M. C_{30} stationary phases for the analysis of food by liquid chromatography. *J. Chromatogr.* **2000**, *880* (1−2), 189–202.

(8) Cámara, M.; Sánchez Mata, M. C. Tomatoes, lycopene and human health. In *Lycopene Analysis in Foods*; Rao, V., Ed.; Caledonian Press: Barcelona, Spain, 2006; Chapter 7, pp 9−62.

(9) Olives Barba, A. I.; Camara Hurtado, M.; Sanchez Mata, M. C.; Fernandez Ruiz, V.; Lopez Saenz de Tejada, M. Application of a UV-vis detection-HPLC method for a rapid determination of lycopene and beta-carotene in vegetables. *Food Chem.* **2006**, *95*, 328–336.

(10) Roldán-Gutiérrez, J. M.; Luque de Castro, M. D. Lycopene: The need for better methods for characterization and determination. *Trends Anal. Chem.* **2007**, *26* (2), 163–170.

(11) Fish, W. W.; Perkins-Veazie, P.; Collins, J. K. A quantitative assay for lycopene that utilizes reduced volumes of organic solvents. *J. Food Compos. Anal.* **2002**, *15*, 309–317.

(12) Cámara, M.; Matallana, M. C.; Sánchez-Mata, M. C.; Lillo, R.; Labra, E. Lycopene and Hydrometilfurfural (HMF) evaluation in tomato products. *Acta Hort.* **2003**, *613*, 365–371.

(13) Torrecilla, J. S.; Mena, M. L.; Yáñez-Sedeño, P.; García, J. A neural network approach based on gold-nanoparticle enzyme biosensor. *J. Chemom.* **2008**, *22*, 46–53.

(14) Torrecilla, J. S.; Fernández, A.; García, J.; Rodríguez, F. Determination of 1-ethyl-3-methylimidazolium ethylsulfate ionic liquid and toluene concentration in aqueous solutions by artificial neural network/UV/vis spectroscopy. *Ind. Eng. Chem. Res.* **2007**, *46*, 3787–3793.

(15) Huang, Y.; Kangas, L. J.; Rasco, B. A. Applications of artificial neural networks (ANNs) in food science. *Crit. Rev. Food Sci.* **2007**, *47*, 113–126.

(16) Zechmeister, L.; LeRosen, A. L.; Schroeder, W. A.; Polgár, A.; Pauling, L. Spectral characteristics and configuration of some stereoisomeric carotenoids including prolycopene and pro-γ-carotene. *J. Am. Chem. Soc.* **1943**, *65*, 1940–1950.
(17) AOAC (Association of Official Analytical Chemists). *Official Methods of Analysis*; AOAC: Arlington, VA, March 1996; Supplement.
(18) Maren, A. J.; Harston, C. T.; Pap, R. M. *Handbook of Neural Computing Applications*; Harcourt Brace Jovanovich, Publishers, Academic Press, Inc.: San Diego, CA, 1990.
(19) Palancar, M. C.; Aragon, J. M.; Torrecilla, J. S. pH-control system based on artificial neural networks. *Ind. Eng. Chem. Res.* **1998**, *37*, 2729–2740.
(20) Himmelblau, D. M. Applications of artificial neural networks in chemical engineering. *Korean J. Chem. Eng.* **2000**, *17*, 373–392.
(21) Torrecilla, J. S.; Mena, M. L.; Yáñez-Sedeño, P.; García, J. Quantification of phenolic compounds in olive oil mill wastewater by artificial neural network/laccase biosensor. *J. Agric. Food Chem.* **2007**, *55*, 7418–7426.
(22) Tetko, I. V.; Livingstone, D. J.; Luik, A. I. Neural network studies. 1. Comparison of overfitting and overtraining. *J. Chem. Inf. Comput. Sci.* **1995**, *35*, 826–833.
(23) Demuth, H.; Beale, M.; Hagan, M. *Neural Network Toolbox for Use with MATLAB® User's Guide*, version 4.0.6, ninth printing revised for version 4.0.6 (release 14SP3); The MathWorks: Natick, MA, 2005.
(24) Torrecilla, J. S.; Aragón, J. M.; Palancar, M. C. Modeling the drying of a high-moisture solid with an artificial neural network. *Ind. Eng. Chem. Res.* **2005**, *44*, 8057–8066.
(25) Ruan, R.; Almaer, S.; Zhang, J. Prediction of dough rheological properties using neural networks. *Cereal Chem.* **1995**, *72*, 308–311.
(26) Sun, Y.; Peng, Y.; Chen, Y.; Shukla, A. J. Application of artificial neural networks in the design of controlled release drug delivery systems. *Adv. Drug Delivery Rev.* **2003**, *55*, 1201–1215.
(27) ICH Guideline Q2B. *Fed. Regist.* **1997**, *62*, 27463−27467.

Received for review February 20, 2008. Revised manuscript received May 7, 2008. Accepted May 15, 2008. We are grateful to the Spanish Ministry of Education and Science for their financial support for Project CTQ2006-04644. J.S.T. is supported by a Ramón y Cajal research contract given by the Spanish Ministry of Education and Science in Spain. G.P. is supported by an undergraduate grant provided by the Spanish Ministry of Education and Science.

JF8005239